Studies on the electronic structure and the elastic properties of the Gd_2SiO_5 crystal with GGA+U approach

HAN ZHANG, TINGYU LIU*, RUILIN SUN, XIAOLI GAO, GUANFANG XIA, KUN TAO[a]
College of Science, University of Shanghai for Science and Technology, Shanghai 200093, China
[a]School of Physical Science and Technology, Lanzhou University, Lanzhou 730000, China

An important optical host material – Gadolinium silicate Gd_2SiO_5 is investigated within the framework of density functional theory and projector-augmented-wave methods. The GGA+U approach has been used to account for the strong on-site Coulomb repulsion among the localized Gd-4f electrons. The effective on-site Coulomb interaction U_{eff} has been examined systematically and is set to 8eV. The calculated elastic properties and refractive index using our chosen parameters are in agreement with the experimental results. This shows that the method and calculation parameters selected in this paper are suitable for studying the Gd_2SiO_5 crystal, which will provide the good base for further investigating the properties of the crystal.

(Received February 20, 2014; accepted January 21, 2015)

Keywords: A: Inorganic compounds, C: Ab initio calculations, D: Electronic structure, D: Elastic properties, D: Optical properties

1. Introduction

Gadolinium silicate Gd_2SiO_5 crystal (GSO) belongs to rare earth orthosilicate crystals which is a good optical host material. GSO crystals doped with impurity ions such as Pr^{3+}, Eu^{3+}, Tb^{3+}, especially Ce^{3+}, are applied as scintillation crystals. Cerium-doped GSO crystal was made for the first time by Takagi using the Czochralski Method. [1] The Ce:GSO scintillator is known to have a very strong radiation resistance, a fast decay time (30 to 60 ns) among inorganic scintillators, non-hygroscopicity, and a large amount of light yield (20% of NaI). On account of these properties, Ce:GSO scintillation crystal is often applied to oil detection image, nuclear medicine (PET) and high-energy nuclear physics. In addition, GSO crystal doped with Yb^{3+} ions may serve as a femtosecond solid laser gain medium. [2] Low symmetry of the crystal structure is more advantageous to the energy level splitting of Yb^{3+}, and so far Yb:GSO is found to be one of the largest energy level splitting in the Ytterbium-doped materials.

Because GSO crystals doped with impurity ions show so many excellent properties, it has attracted an increasing attention. Over the past decade, there are a lot of experiments and studies on GSO doping, which mainly concentrate on how to improve the performance of impurity ions-doped GSO crystal experimentally. [3-5] However, first principle study on host material-GSO crystals is sparse, especially for calculations of impurity ions doped GSO. On the contrary, lots of studies have been done on LSO (Lu_2SiO_5) and YSO (Y_2SiO_5), which also belong to rare-earth silicate. The lack of literature information on quantum-chemical calculations of GSO might make it impossible to analyze experiment phenomenon from the microcosmic point of view, and the theoretical study of perfect GSO crystals is the foundation of further studying the doping mechanism. Therefore, the first principle calculation of the GSO crystal is particularly important.

In the crystal shell Gd-4f orbital is half filled, so the GSO is a strong correlation system, which brings some troubles in computation. Density functional theory (DFT) is recognized as one of the most commonly used method in physical and chemical fields. However, there are few literatures about calculation of GSO crystal till now. In this paper, the DFT+U approach for the strong correlation system will be employed in the calculation [6-8]. The electrons are divided into two sub-systems: s and p electrons are processed by the local density approach (LDA) or generalized gradient approach (GGA). And d and f electrons are treated with the Hubbard parameter U which reflects the strength of the on-site Coulomb interaction, and the exchange term J has also been taken into consideration. In this paper, we have investigated the electronic structure, elastic properties and refractive index of the perfect GSO crystal by first principle calculations within GGA+U approach, aiming at providing the reference for the theoretical research about GSO crystal.

2. Theories and methods

2.1. Crystal structure

The geometry structure of GSO is shown as Fig. 1.

Single crystalline Gd_2SiO_5 is monoclinic, characterized by symmetry group $P2_1/c$ with lattice parameters a = 9.12 Å, b = 7.06 Å, c = 6.73 Å, β = 107.35°, [9] and it has four molecular units that is 32 atoms in the primitive cell. As shown in Fig. 2, there are five kinds of oxygen ions in different sites, marked as O1, O2, O3, O4, and O5. Gd ions are coordinated by nine and seven oxygen ions respectively, marked as Gd1 and Gd2. Gd1 is bonded to one isolated oxygen ion (O5), and to six tetrahedral $[SiO_4]^{4-}$ ions through two oxygen atoms in two cases and through one oxygen atom in four cases. Gd2 is bonded to three isolated oxygen ions (O5), and to three tetrahedral $[SiO_4]^{4-}$ ions through two oxygen atoms in one case and through one oxygen atom in two cases.

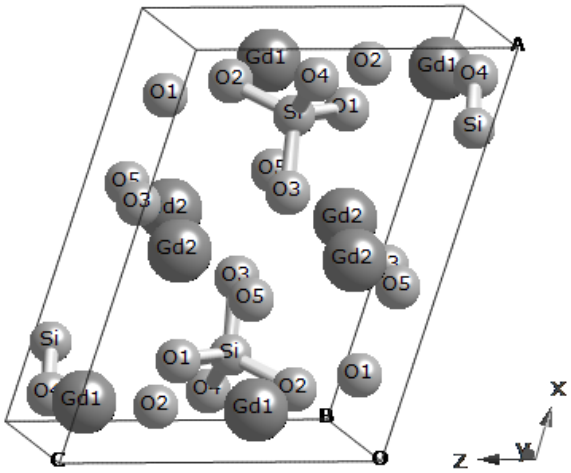

Fig. 1. The crystal structure of GSO crystal.

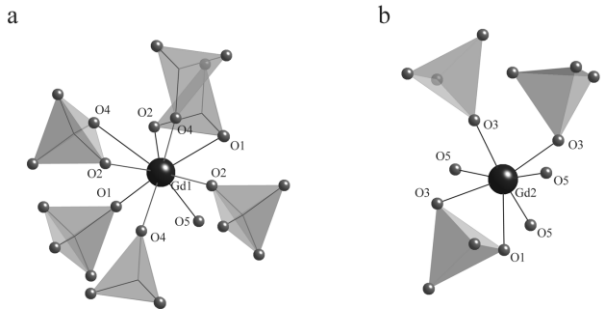

Fig. 2. Local coordination structures of two gadolinium (Gd1 (a) and Gd2 (b)) sites in GSO.

2.2. Calculation methods

In this paper, all first principles calculations of perfect GSO crystal have been performed with the Vienna Abinitio Simulation Package (VASP) based on density functional theory (DFT) and the projector augmented wave (PAW) method. The electronic exchange-correlation potentials are described with generalized gradient approximation (GGA) of Perdew–Burke–Ernzerhof (PBE). [10] Gd （4f7 5s2 5p6 5d1 6s2）, Si （3s2 3p2）, O（2s2 2p6） are explicitly treated as valence electrons. Owing to half full 4f electrons, the GGA+U approach is used. The form of the total GGA energy functional is given as follow:

$$E_{GGA(LDA)+U} = E_{GGA(LDA)} + \frac{U-J}{2}\sum_{\sigma}[Tr\rho^{\sigma} - Tr(\rho^{\sigma}\rho^{\sigma})]$$

in which U is the spherically averaged screened Coulomb energy and J is the exchange energy.

In this paper, effective on-site Coulomb interaction U_{eff}=U-J method by Dudarev's approach is employed. [11] The exchange term J is fixed as 1eV. The U_{eff} value is inferred from the band gaps and the energy difference between the occupied state and unoccupied state of Gd-4f electrons as a function of U_{eff} from 0eV to 9eV. After a series of convergence tests for different plane-wave energy cutoff and k-point sampling, the plane-wave energy cutoff is set to 550eV and the k-points mesh is set to 2×3×3 in the reciprocal space K. Ground state geometries are optimized until the Hellman-Feynman forces on each atom are less than 0.02eV/Å and the energy converged to $1x10^{-6}$eV. All other calculations are based on the optimized geometries.

3. Results and discussions

3.1. Effective on-site Coulomb interaction U_{eff}

To calculate the ground-state properties correctly, in general, the semi-experiential parameter U_{eff} was determined from the following several aspects: (1) the band gap. (2) the energy difference (ΔE) between the occupied state and unoccupied state of Gd-4f electrons. (3) the results of the geometry optimization. This method has been successfully used in the calculation of $GdTaO_4$ crystal by Gu et al. [12].

The energy difference of spin-up state and spin-down state of Gd-4f electrons were read out from density of states, which were calculated using different U_{eff} from 0 to 9. The spin-up state of Gd-4f electrons is occupied by electrons, which is called the occupied state. The spin-down state of Gd-4f electrons is unoccupied, called the unoccupied state. The energy difference between the occupied state and the unoccupied state of Gd-4f electrons is shown in Fig. 3. With the increase of U_{eff} values, the energy of the spin-down electrons move upwards, and the energy of the spin-up electrons move downwards, causing the energy difference to increase linearly. The Gd-4f electron orbital is shielded by 5s2 and 5p6 electrons, they do not contribute significantly to chemical bonds, so the energy difference of 4f in different materials may be negligible. Experiments found that the energy difference

of the occupied state and the unoccupied state of Gd-4f electrons in gadolinium materials is commonly between 12eV and 13.5eV [8,13,14].

For U_{eff} between 6eV and 9eV, the energy difference (ΔE) is within the range of 12eV to 13.5eV. The ΔE corresponding to U_{eff}=7 and U_{eff}=8 are calculated to be 12.35eV and 13.39eV, respectively. And for U_{eff}=6eV and U_{eff}=9eV, the ΔE are 11.30eV and 14.32eV, respectively, where the former is less than the experimental value and the latter is greater than the experimental value. From the band gap aspect, the band gap remains 4.66eV when U_{eff} is larger than 4eV, as shown in Fig. 4. When U_{eff} is less than 4eV, Gd-4f band is located in the forbidden band, which is contrary to experimental facts.

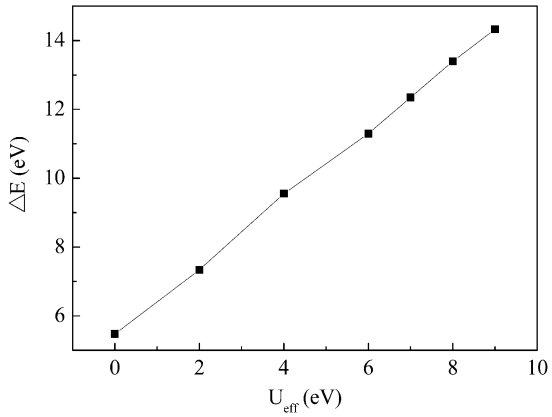

Fig. 3. Energy difference between the occupied state and unoccupied state of Gd-4f electrons as a function of U_{eff}.

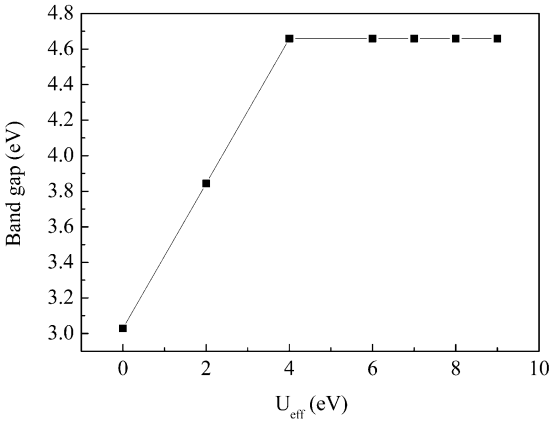

Fig. 4. Band gap as a function of U_{eff}.

Comparing geometry optimization results for U_{eff}=7 with that for U_{eff}=8, it can be seen that the optimized structure for U_{eff}=8 is much closer to the experimental value and relative error below 1.0%, summarized in Table 1. Therefore, the value of U_{eff} is set as 8eV for all calculations. It's worth mentioning that the appreciate U_{eff} in this paper is the same with $GdTaO_4$ crystal calculated by Gu, by extension, U_{eff}=8eV is probably the appreciate value of crystals which contain Gd^{3+}.

Table 1. Equilibrium structure parameters at U_{eff}=7 eV, U_{eff}=8 eV and experimental values of GSO.

	a (Å)	b (Å)	c (Å)	β	Volume(Å^3)
Experiment [9]	9.12	7.06	6.73	107.35°	414
U_{eff}=7 eV	9.222	7.126	6.793	107.5°	425.7
U_{eff}=8 eV	9.22	7.125	6.792	107.5°	425.5

3.2 Electronic structures

The band structure of GSO has been obtained along the high-symmetry lines of the first Brillouin zone, as shown in Fig. 5. The bottom of conduction band (CB) is obviously at Γ point, and the top of the valance band (VB) is very flat. So the gap in this crystal can be considered as a direct band gap, which is very similar to the band structure of the YSO (Y_2SiO_5) crystal calculated with the OLCAO method. [15] Our calculated direct gap is 4.66eV. We find no reported experimental data for the gap, however, the band gap of GSO:Ce with a value of 6.1eV measured by Rachko [16] can be approximately equal to the gap of the perfect GSO crystal. Our calculated gap is less than the real gap because of a well-known problem that GGA or LDA theory generally underestimates the band gaps of semiconductors and insulators. A quantity of local bands 6.44eV below the VB and the same local bands 2.24eV above the CB are the spin-up state and the spin-down state of Gd-4f electrons respectively, and the energy difference is 13.39 eV. This phenomenon does not exist in the band structure of YSO and LSO since the Y-4f electrons and Lu-4f electrons are fully optimized.

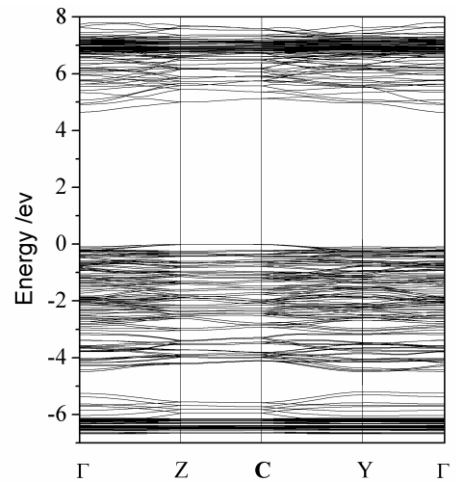

Fig. 5. Calculated band structure of GSO.

Based on the optimized structure, we calculated the density of state (DOS) and partial density of state (PDOS) of GSO by adding k-point mesh to 4×6×6. Fig. 6 and Fig. 7 show the DOS and PDOS of GSO respectively. Two sharp peaks located at the flank of the -40eV are spin-down states and the spin-up states of Gd-5s. From the

amplification of illustration, it can be found that the two sharp peaks just mentioned split into two new sharp peaks with the same spin respectively. These two peaks are made of Gd1-5s states and Gd2-5s states, and there is an energy difference with 0.187eV between them which is due to those two kinds of Gd ions with coordination numbers 7 and 9 would be affected by two kinds of ligand field although Gd-5s electrons are shielded by 5p electrons. It is worth mentioning that the Gd-4f electrons have the same phenomenon. The area from -22eV to -15eV can be called a core zone, mainly made by Gd-5p states and O-2s states. The VB DOS can be divided into two regions. Those states from -5eV to 0eV are mainly made of O-2p and Si-3p states, and local Gd-4f states are located near the bottom of the VB. The CB is in the range of 4.6eV to 7eV, dominantly made by Gd-5d states and the spin-down states of Gd-4f and few states of Si-3p.

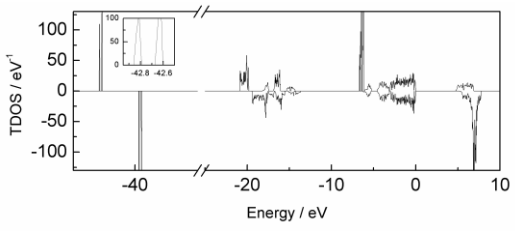

Fig. 6. Total density of states in GSO. The inset shows 5p states of Gd1 (Gd1-5s) and Gd2 (Gd2-5s).

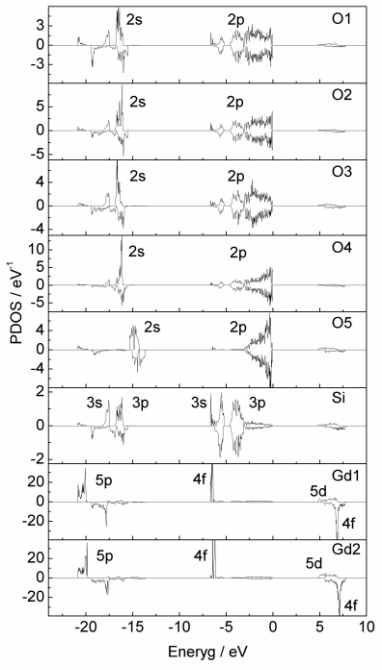

Fig. 7. Partial density of states in GSO.

From the PDOS we can also get the following information: (1) The PDOS of the O5 does not overlap with that of the Si atoms, which is totally different from the PDOS of the other four O atoms, because the O5 is not bonded to any Si atom. (2) The PDOS of O1, O2, O3 and O4 are very similar to each other and heavily overlap with the PDOS of the Si atom. Interactions between the O-2p electrons and the valence electrons of the Si atom can be considered to be bonded at the bottom of the VB, and to be anti-bonded in the CB. (3) There is a very strong peak of the Gd-4f states near the bottom of the VB, and it is a non-bonding due to the shielding of the 5s and 5p electrons. Therefore, due to this reason, sharp lines were observed in the absorption spectra of the GSO [17] and other crystals contained with Gd^{3+}, which suggests that it arise from the transitions in the core excitons formed by the 4f-4f transitions of Gd^{3+} [18].

In order to observe the electronic structure visually, the charge density of GSO in the (0 0 1) plane and (1 0 0) plane are obtained, as shown in Fig. 8. From Fig. 8 (a), it can be seen clearly that there are overlaps of electron cloud between the Si atom and O3 atom, the Si atom and O4 atom, and obvious directivity of the valance electron's charge distribution of O3 atom and O4 atom. This illustrates that the chemical bond of Si-O3 bond and Si-O4 bond is a typical covalent bond. It can be seen that charge distribution around the Gd2 and O5 atoms is isolated. This illustrates that the chemical bond between the Gd2 and O5 atoms is an ionic bond. Similarly, the Si-O1 bond and Si-O2 bond in Fig. 8 (b) are also covalent bonds. Compare the above two figures comprehensively, we may safely draw the following conclusion: (1) The O1, O2, O3, O4 and Si atoms form a tetrahedron structure, and the Si atom is in the center of the tetrahedron, and the Si-O chemical bonds of the tetrahedron is a covalent bond with the sp3 hybridization similar as that of CH_4. (2) Ionic bonds are formed between the Gd atom and O5 atom, the Gd atom and SiO_4 groups. The above conclusions are consistent with the results of the DOS and band structure.

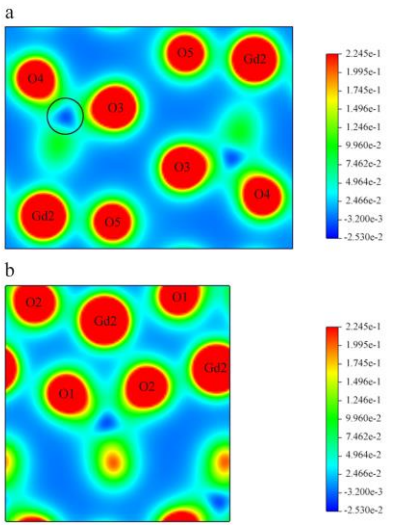

Fig. 8. Charge density of GSO in the (0 0 1) plane and (1 0 0) plane are plotted in (a) and (b). The black circle indicates the overlap of electron cloud between the Si atom and the neighboring O atom.

3.3 Elastic properties

Elastic properties of GSO single crystal were obtained within the framework of the VASP calculations. The elastic tensor is determined by performing six finite distortions of the lattice and deriving the elastic constants from the strain-stress relationship. [19] The GSO is classified as a monoclinic class 2/m single crystal, and has strong anisotropy in the elastic constants. There are thirteen independent elastic stiffness constants in a monoclinic, and the elastic stiffness constant matrix is shown as follows.

$$\left[C_{ij}\right] = \begin{bmatrix} C_{11} & C_{12} & C_{13} & 0 & C_{15} & 0 \\ & C_{22} & C_{23} & 0 & C_{25} & 0 \\ & & C_{33} & 0 & C_{35} & 0 \\ & & & C_{44} & 0 & C_{46} \\ & sym. & & & C_{55} & 0 \\ & & & & & C_{66} \end{bmatrix}$$

Table 2 lists the calculated values of the elastic constants and the experimental values measured using ultrasonic pulse method by Kazuhisa Kurashige [20].

Table 2. Calculated elastic constants C_{ij} (in Gpa) compared to experimental results of GSO.

Properties	Calculated	Experimental[20]
C_{11}	194.5	223
C_{12}	95.5	108
C_{13}	103.8	98.5
C_{15}	4.7	8.4
C_{22}	121.4	150
C_{23}	127	102
C_{25}	14.9	33.3
C_{33}	225	251
C_{35}	-8.9	-6
C_{44}	74.3	78.8
C_{46}	4.7	6.6
C_{55}	62.3	68.8
C_{66}	74.7	82.7

From the comparison, it is found that several key parameters C_{11}, C_{12}, C_{13}, C_{22}, C_{23}, C_{33}, C_{44}, C_{55} and C_{66} are in agreement with the experimental data. Based on these key parameters, we can further investigate the anisotropic characters and other elastic properties.

The shear anisotropic factors on different crystallographic planes provide a quantitative measure of the degrees of anisotropy in atomic bonding in different planes. [21] The shear anisotropic factors on the (1 0 0), (0 1 0) and (0 0 1) planes are given by

$$A_1 = \frac{4C_{44}}{C_{11} + C_{33} - 2C_{13}} \quad (1)$$

$$A_2 = \frac{4C_{55}}{C_{22} + C_{33} - 2C_{23}} \quad (2)$$

$$A_3 = \frac{4C_{66}}{C_{11} + C_{22} - 2C_{12}} \quad (3)$$

The calculated values of A_1, A_2 and A_3 are 1.4, 2.7 and 2.4, respectively. We can clearly see that, the shear anisotropic factors on the (0 1 0) plane and (0 0 1) plane are very similar, and absolutely different from that of the (1 0 0) plane. Hence, GSO exhibits anisotropy, and the degree of anisotropy in the (0 1 0) plane and (0 0 1) plane are very close.

The bulk (K) and shear (G) moduli can be obtained using the Voigt method, [22] the Reuss method [23] and the Hill method. [24] The equations of Voigt and Reuss approximations are given as follows:

$$K_V = \frac{1}{9}(C_{11} + C_{22} + C_{33} + 2(C_{12} + C_{13} + C_{23})) \quad (4)$$

$$K_R = (S_{11} + S_{22} + S_{33} + 2(S_{12} + S_{13} + S_{23}))^{-1} \quad (5)$$

$$G_V = \frac{1}{15}(C_{11} + C_{22} + C_{33} + 2(C_{44} + C_{55} + C_{66}) - C_{12} - C_{13} - C_{23}) \quad (6)$$

$$G_R = \frac{15}{4(S_{11} + S_{22} + S_{33} - S_{12} - S_{13} - S_{23}) + 3(S_{44} + S_{55} + S_{66})} \quad (7)$$

in which the subscripts V and R indicate the Voigt method and the Reuss method, respectively. The S_{ij} is the elastic compliance constant matrix and has the following relationship with the elastic stiffness constant matrix:

$$S_{ij} = \left[C_{ij}\right]^{-1} \quad (8)$$

Experimental results of the bulk and shear moduli are generally given by the Hill method, which is the average of the calculated values of the other two methods mentioned above. The averages are given by

$$G = \frac{1}{2}(G_R + G_V) \qquad K = \frac{1}{2}(K_R + K_V) \quad (9)$$

The Young's moduli (E) and the Poisson ratio (v) can be calculated using the relationship:

$$E = \frac{9KG}{3K + G} \quad (10)$$

$$v = \frac{3K - 2G}{2(3K + G)} \quad (11)$$

The bulk moduli, shear moduli, Young's moduli and

Poisson ratio for GSO are calculated using Eqs.(4)-(11), and the results are presented in table 3. Due to lack of the experimental data, instead, we calculated these constants using Eqs.(4)-(11) with the elastic stiffness constant matrix given by experiment listed in Table 2. Compared two computing results, we believe that the calculated values are reasonable and reliable.

Form the B/G ratio, we can see the brittleness and ductility of the materials. A higher value of B/G indicates a better ductility of the material. According to the criterion, [25, 26] the value to distinguish between the brittleness and ductility is 1.75. The calculated value of B/G is higher than 1.75. Therefore, the GSO crystal has a good ductility.

The Poisson ratio reflects the size of volume change in the uniaxial deformation of a material. The theoretical maximum of Poisson ratio is 0.5, which indicates no volume change. Typical values for many materials lie in the range of 0.2-0.3. Our calculated Poisson ratio is 0.35, which is very close to the experimental value of YSO crystal listed in Table 3. This indicates that the volume of GSO and YSO crystals change very little in the uniaxial deformation.

Table 3. Calculated and experimental values of bulk moduli B, shear moduli G, Young's moduli E (in Gpa) and Poisson ration of GSO and YSO crystals.

Properties	GSO	YSO
B_V	132.6[a]	
	132.9[b]	
B_R	111.9[a]	
	124.3[b]	
B	122.25[a]	108[c]
	128.6[b]	
G_V	42.48[a]	
	48.74[b]	
G_R	36.38[a]	
	53.76[b]	
G	39.43[a]	47[c]
	51.39[b]	
B/G	3.1[a]	2.3[c]
	2.5[b]	
E	106.8[a]	124[c]
	136[b]	
v	0.35[a]	0.31[c]
	0.31[b]	

[a]This work.

[b]Calculated using Eqs.(4)-(11) with the elastic stiffness constant matrix given by experimental data from Ref. [20]

[c]Exp. In Ref. [27]

3.4. Refractive index

The static dielectric matrix is calculated based on density functional perturbation theory. The usual expressions in perturbation theory

$$\nabla_k \left| u_{nk} \right\rangle = \sum_{n' \neq n} \frac{\left| u_{n'k} \right\rangle \left\langle u_{n'k} \right| \frac{\partial (H(k) - \varepsilon_{nk} S(k))}{\partial k} \left| u_{nk} \right\rangle}{\varepsilon_{nk} - \varepsilon_{n'k}} \quad (12)$$

are rewritten as linear Sternheimer equations:

$$(H(k) - \varepsilon_{nk} S(k)) \left| u_{nk} \right\rangle = -\frac{\partial (H(k) - \varepsilon_{nk} S(k))}{\partial k} \left| u_{nk} \right\rangle \quad (13)$$

According to Sternheimer theory, the static dielectric constant ε is calculated as shown in Table 4. From the relationship between the refractive index and dielectric constant $n = \sqrt{\varepsilon}$, the refractive index of GSO single crystal in the x, y and z directions are calculated and the results are listed in Table 4. The average refractive index, which has been calculated to be 1.96 is considered reasonable due to its small variance in three directions. This value is very close to the experimental value 1.85 [28]. It is showing that GSO crystal has a relative low refractive index.

Table 4. Static dielectric constant and refractive index in the x, y and z directions.

Properties	ε_{xx}	ε_{yy}	ε_{zz}	n_{xx}	n_{yy}	n_{zz}
Calculated	3.805	3.835	3.911	1.95	1.96	1.98

4. Conclusions

The electronic structures, elastic properties and refractive index of Gd_2SiO_5 crystal have been investigated within the GGA+U frameworks, which can be concluded at following:

(1) The band gap, energy difference between spin-up and spin-down states of Gd-4f electrons, and lattice parameters have been studied as a function of the effective on-site Coulomb interaction parameter U_{eff}. The most appropriate value of U_{eff} is proved to be 8eV.

(2) The calculated electronic structures show that the GSO crystal has a 4.66eV direct gap and the bottom of CB is at Γ point. Analysis of the DOS and PDOS reveals that the VB is consisted with O-2p and Si-3p states, the

CB is composed of Gd-5d and Gd-4f, and the O-2p and Gd-5d states are located at the top of VB and the bottom of CB, respectively.

(3) The thirteen independent elastic constants of monoclinic GSO crystal have been calculated. Nine key parameters C_{11}, C_{12}, C_{13}, C_{22}, C_{23}, C_{33}, C_{44}, C_{55} and C_{66} of the thirteen constants are in agreement with the experimental data. According to nine parameters, the anisotropic characters and other elastic properties are investigated.

(4) The refractive index of GSO is calculated to be 1.96, which is very close to the experimental data.

Acknowledgements

This work is supported by the Hujiang Foundation of China (B14004).

References

[1] K. Takagi, T. Fukazawa, Appl. Phys. Lett. **42**, 43 (1983).
[2] C. F. Yan, G. J. Zhao, L. B. Su, X. D Xu, L. H, Zhang, J. Xu, J. Phys.: Condens. Matter **18**, 1325 (2006).
[3] M. Y. Jie, G. J. Zhao, X. H. Zeng, L. B. Su, H. Y. Pang, X. M. He, J. Xu, J. Cryst. Growth. **277**, 175 (2005).
[4] V. Bondar, B. Grinyov, K. Katrunov, L. Lisetski, L. Nagornaya, V. Ryzhikov, V. Spasov, N. Starzhinskiy, G. Tamulaitis, Nucl. Instrum. Meth. A **537**, 215 (2005).
[5] V. G. Bondar, B. P. Tsapenko, A. B. Tsapenko, Functional Materials. **17**, 217 (2010).
[6] M. Richter, J. Phys. D **31**, 1017 (1998).
[7] V. I. Anisimov, F. Aryasetiawan, A. I. Lichtenstein, J. Phys.: Condens. Matter **9**, 767 (1997).
[8] V. I. Anisimov, J. Zaanen, O. K. Andersen, Phys. Rev. B **44**, 943 (1991).
[9] N. A. Toropov, I. A. Bondar, A. N. Lazarev, Yu. I. Smolin, Silicates of Rare-earth Elements and their Analogs, Nauka, Leningrad, (1971); Yu. I. Smolin, S. P. Tkachov, Sov. Phys. Crystallogr. **14**, 14 (1969).
[10] J. P. Perdew, K. Burke, M. Ernzerhof, Phys. Rev. Lett. **77**, 3865 (1996).
[11] S. L. Dudarev, G. A. Botton, S. Y. Savrasov, C. J. Humphreys, A. P. Sutton, Phys. Rev. B **57**, 1505 (1998).
[12] M. Gu, L. Lin, B. Liu, X. L. Liu, S. M. Huang, C. Ni, Acta Phys. Sin. **59**, 2836 (2010).
[13] V. N. Antonov, B. N. Harmon, A. N. Yaresko, A. P. Shpak, Phys. Rev. B **75**, 184422 (2007).
[14] Y. Hajime, F. Tadashi, M. Takayuki, T. Yoshiki, I. Shin, S. Shigemass, D. X. Li, S. Takashi, J. Phs. Soc. Jpn. **65**, 1000 (1996).
[15] W. Y. Ching, L. Z. Ouyang, Y. N. Xu, Phys. Rev. B **67**, 245108 (2003).
[16] Z. A. Rochko, I. A. Tale, V. D Ryzhikov, J. L. Jansons, S. F. Burochas, Nuclear Tracks and Radiation Measurements. **21**, 121 (1993).
[17] K. Mori, M. Nakayama, Phys. Rev. B **67**, 165206 (2003).
[18] H. M. Crosswhite, R. L. Schwiesow, J. Chem. Phys. **50**, 5032 (1969).
[19] Y. L. Page, P. Saxe, Phys. Rev. B **65**, 104104 (2002).
[20] K. Kurashige, Y. Kurata, H. Ishibashi, K. Susa, Jpn. J. Appl. Phys. **36**, 2242 (1997).
[21] K. B. Panda, K. S. Ravi Chandran, Acta Materialia. **54**, 1641 (2006).
[22] W. Voigt, Lehrburck der kristallphysik, Teubner, Leipzig (1928).
[23] A. Reuss, Z. Angew, Math. Mech. **9**, 49 (1929).
[24] R. Hill, Proc. Phys. Soc. London, **65**, 350 (1952).
[25] I. R. Shein, A. L. Ivanovskii, J. Phys.: Condens. Matter **20**, 415218 (2008).
[26] S. F. Pugh, Philos. Mag. **45**, 833 (1954).
[27] Z. Q. Sun, J. Y. Wang, M. S. L, Y. C. Zhou, J. Eur. Ceram. Soc. **28**, 2895 (2008).
[28] M. Kobayashi, K. Takamatsu, S. Ide, K. Mori, S. Sugimoto, H. Takaki, M. Yuasa, M. Ishii, Nucl. Instr. and Meth. **A306**, 139 (1991).

*Corresponding author: liutyyxj@163.com